ELSEVIER

Journal of Molecular Catalysis A: Chemical 117 (1997) 455–469

JOURNAL OF MOLECULAR CATALYSIS A: CHEMICAL

New dioxomolybdenum(VI) catalysts for the selective oxidation of terminal *n*-alkenes with molecular oxygen

Wolfgang A. Herrmann [a,*], Gerhard M. Lobmaier [a], Thomas Priermeier [a], Mike R. Mattner [a], Bernd Scharbert [b]

[a] *Anorganisch-chemisches Institut der Technischen Universität München, Lichtenbergstrasse 4, 85747 Garching bei München, Germany*
[b] *Hoechst AG, Central Research Laboratories, 65926 Frankfurt am Main, Germany*

Received 19 April 1996; accepted 5 September 1996

Abstract

New dioxomolybdenum(VI) complexes of the type MoO_2L_2 [L = (2′-pyridyl)alcoholate] are able to change considerably the product distribution of the *metal catalyzed* autoxidation process. With the catalyst bis[*N,O*-{(2′-pyridyl)pentan-3-olato}]dioxomolybdenum(VI) (**2**) the epoxide is formed as the main product in the autoxidation process of 1-octene. The product selectivity is increased from 24% (epoxide, autoxidation) to 58% upon treatment of 1-octene with molecular oxygen (1 bar and 100°C) in the presence of **2**. An additional advantage is that the catalyst can be recovered. The synthesis and the characterization of the new dioxomolybdenum(VI) complexes and the ligands is described in addition to their catalytic properties. The structure of the new complex bis[*N,O*-{(2′-pyridyl)pentan-3-olato}]dioxomolybdenum(VI) (**2**) was determined by X-ray diffraction: monoclinic space group P $2_1/c$, $a = 1444.5(2)$ pm, $b = 1052.4(1)$ pm, $c = 1511.5(2)$ pm, $\beta = 115.86(1)°$, $V = 2068(1) * 10^6$ pm^3. The epoxidation data indicate an important influence of the ligand sphere of the catalyst on the product distribution. We have now the possibility of fine tuning the complexes in the metal catalyzed autoxidation reaction.

Keywords: Catalysis; Oxidation; Olefins; Epoxides; Molybdenum

1. Introduction

The oxidation of terminal olefins to the corresponding epoxides by means of *molecular oxygen* constitutes one of the great challenges in catalysis [1,2]. Most important oxygen containing bulk chemicals are produced with molecular oxygen as oxidant, with only few exceptions, for example propylene oxide [3,4]. There are now ruthenium porphyrin catalysts available that effect catalytic oxidation of terminal olefins [5,6]. The disadvantages, however, are rapid, mostly unknown decomposition pathways for which reason they are not high-rated candidates for industrial processes [7]. There is a non-catalytic way to oxidize olefins (even propene) with molecular oxygen, commonly referred to as 'olefin autoxidation'. The limiting product selectivity (ef. in Section 2.3) is ca. 40% for propylene

* Corresponding author.

PII S1381-1169(96)00381-0

oxide under high-pressure conditions [8]. Schnurpfeil et al. have reported that high-valent transition metal oxides or their acetylacetonate derivatives increase the product selectivity of 1-octene oxide in the autoxidation process. For $MoO_2(acac)_2$ and 1-octene an increase in selectivity from 24% at 110°C and 1 bar up to 38% was obtained, thus entering a catalytic path [9,11]. These authors further report that there is no influence of ligand variations on selectivity data. Kelly et al. discovered that ethylene is converted catalytically to ethylene oxide in 69% yield by virtue of MoO_2(8-hydroxyquinoline)$_2$ at an ethylene/oxygen pressure of 90 bar and at 90°C [10]. The present publication presents new oxidation catalysts for 1-octene with elemental oxygen at atmospheric pressure.

2. Results and discussion

2.1. Synthesis of the ligands

For the design of ligands for oxidation catalysis, three prerequisites are to be met: (a) resistance against oxidation, (b) a straight-forward synthetic route and (c) the possibility to change electronic and steric characteristics by simple variation of the starting materials [13]. These principles are combined in the following synthesis. First, the synthesized ligands **1a–8a** are tertiary alcohols, which resist oxidation. Second, the ligands can be made in a simple two-step synthesis: After lithiation of 2-bromopyridine at the *ortho* position the resulting organometallic species undergoes a nucleophilic attack at the carbonyl group of the ketone followed by the protonation of the resulting lithium salt (Eq. (1) and Eq. (2)) [14].

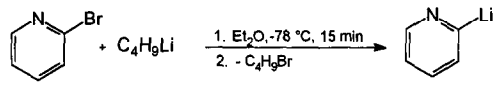

(1)

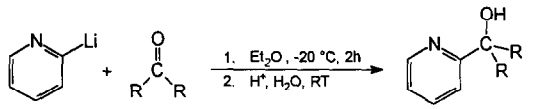

(2)

Third, steric and electronic characteristics can be generated by the use of various symmetric ketones, thus avoiding the creation of new stereocenters in the ligand sphere of the obtained complexes. On this route the alcohols **1a** to **8a** were synthesized (Table 1).

Table 1
Reaction of selected ketones with 2-pyridyllithium

Used ketone	Resulting alcohol	No.
Propan-2-one	(2′-pyridyl)propan-2-ol	**1a**
Pentan-3-one	(2′-pyridyl)pentan-3-ol	**2a**
Heptan-4-one	(2′-pyridyl)heptan-4-ol	**3a**
2,4-Dimethylpentan-3-one	(2′-pyridyl)-2,4-dimethylpentan-3-ol	**4a**
Nonan-5-one	(2′-pyridyl)-4-nonanol	**5a**
Cyclohexanone	1-(2′-pyridyl)cyclohexanol	**6a**
Benzophenone	1,1-diphenylmethanol	**7a**
4,4-′Di-*tert*-butylbenzophenone	1-(2′-pyridyl)-1,1-di((4″-*tert*-butyl)phenyl)methanol	**8a**

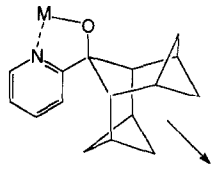

Fig. 1. Steric demand of ligand **6a**.

The deprotonated alcohols can be described as chelating, anionic, bidentate ligands. They complex a metal center with a coordinative bond by the nitrogen of the pyridine ring and a covalent single bond by the alcoholate oxygen of the former hydroxyl group. An additional advantage of these ligands is the number of the ring atoms in the corresponding complex. Five-membered rings are generally thermodynamically more stable than the six-membered rings. At this point, the interest should be focused on ligand **6a**, which is made from cyclohexanone and the lithiated pyridine species. This ligand structurally resembles a mixture of alkyl- and aryl-substituted ligands due to loss of free rotation. This ligand is bulky but sterically directed, when bound to a metal center (Fig. 1).

2.2. Synthesis of the dioxomolybdenum(VI) complexes

The synthesis of the metal complexes, later used for catalytic epoxidation, is based on the starting material $MoO_2(acac)_2$ (**10**) [15,16]. After a simple ligand exchange reaction (Eq. (3)) with the pyridyl alcohols **1a–8a**, (ef.) in Section 2.1) and 2-pyridylmethanol (**9a**), the corresponding molybdenum complexes **1–9** are obtained in high yields.

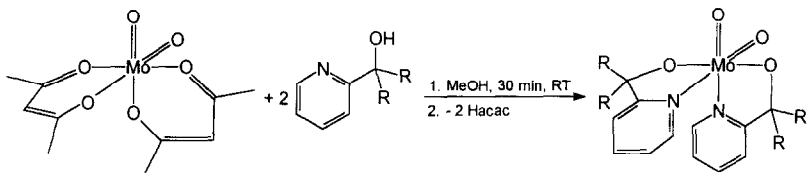

(3)

The driving force of the ligand exchange reaction are different chelating effects. First, the chelating effect of *N,O*-ligands, as compared with *O,O*-ligands, is stronger due to the different bonding energies. Second the complexes **1–9** form a stable five-membered ring chelate. This was shown by GC-MS reaction control. Shortly after addition of the *N,O*-ligand to the methanolic suspension of **10**, no ligand and only the protonated acetylacetone is found.

Contrary to the work of Holm et al., who worked on aryl substituted pyridylthio- and pyridylalcoholate-dioxomolybdenum(VI) complexes [12,17], we focused our synthetic work on the alkyl-substituted alcohols to generate new electronic and steric characteristics [18]. An important aspect is the much better *solubility* of the new complexes in non polar aprotic solvents like alkanes or alkenes, which is important for catalytic applications (Scheme 1).

To study the steric and electronic influence in oxidation catalysis, we have also synthesized the known complexes **7–9** with R = H, phenyl and 4′-*tert*-butylphenyl.

Table 2 summarizes the important spectroscopic data.

All ^{13}C NMR spectra show the striking shift of the signal of the quarternary carbon atom related to the hydroxy function and the pyridine ring. For example, when the ligand is bound to the dioxomolybdenum core, the signal shifts from 75.07 in **2a** to 90.19 ppm in **2**. This can be explained by a shift of electron density towards the molybdenum center. Another indicative chemical shift value

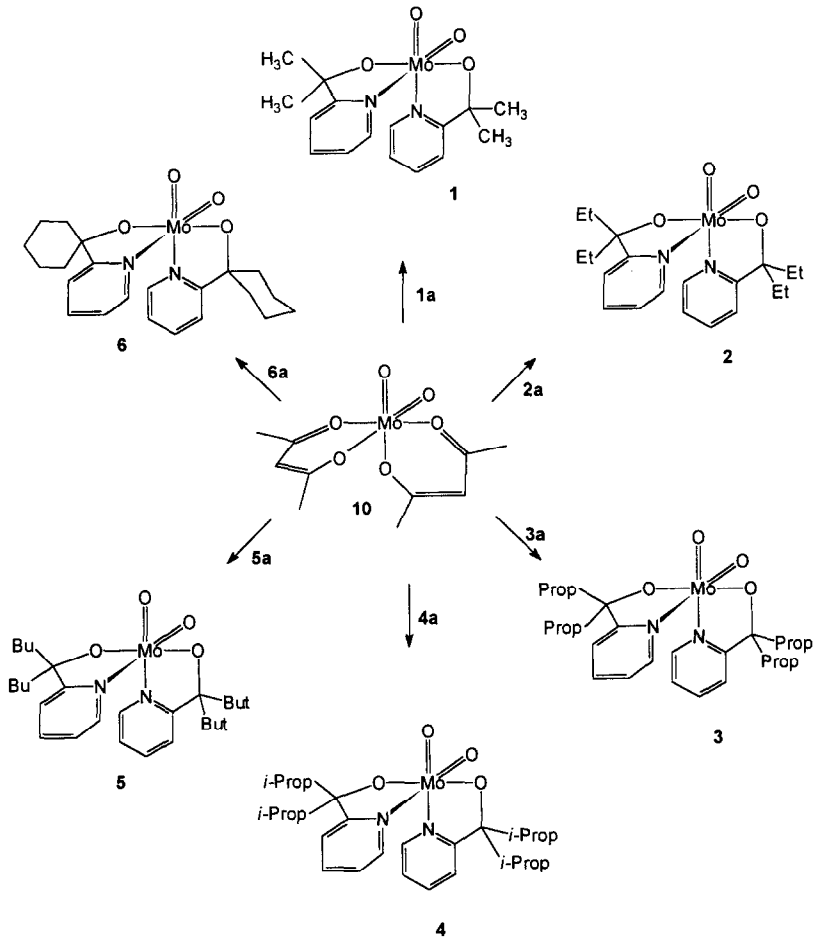

Scheme 1.

is due to the signal of the 2′-carbon of the pyridine ring that can be found at ca. 170 ppm (metal complex). The signal of this carbon nucleus is found at ca. 160 ppm (free ligand). This effect also reveals an electron density shift from the aromatic ring to the molybdenum center.

^{17}O and ^{95}Mo NMR spectra of selected complexes have also been recorded (Table 3). The obtained ^{17}O NMR data of the dioxo atoms are in the expected range of the $[MoO_2]^{2+}$ moiety [19,20]. The known value for the dioxo group of **10** is also given in Table 2 for reasons of comparison [21]. ^{17}O

Table 2
Chemical shifts for the ortho H and the β-H of free ligand and complex

	δ of ortho H (ppm)	δ of ortho H (ppm)	δ of beta H (ppm)	δ of beta H (ppm)
1a, 1	8.50	8.68	1.55	1.78
2a, 2	8.52	8.74	1.84	2.02
3a, 3	8.50	8.69	1.85	2.10
4a, 4	8.52	8.78	2.30	2.45
5a, 5	8.50	8.72	1.80	2.21
6a, 6	8.48	8.62	2.00	2.11

Table 3
^{17}O and ^{95}Mo chemical shifts of complexes **1**, **2**

	^{17}O (ppm)	ν (Hz)	^{95}Mo (ppm)	ν (Hz)
1	895	280	37	250
2	899	270	48	250
MoO_2acac_2	1037	200	3	—
MoO_2q_2	—	—	58	130

q = hydroxyquinoline.

NMR resonances of the hydroxy function could not be detected, probably due to severe exchange broadening.

^{95}Mo chemical shifts of *cis*-dioxomolybdenum(VI) compounds are sensitive to minor ligand variations [22]. The chemical shifts of $MoO_2(SCMe_2CMe_2NHR)_2$ (R = H, CH_3), for example, differ by 129 ppm [23]. MoO_2q_2 (q = 8-hydroxyquinoline), as an example for the *N,O*-substitution pattern, shows a ^{95}Mo resonance within the same region as **1** and **2** (Table 3). The chemical shift difference of **1** and **2** cannot be rationalized by simple electron donation correlation.

The IR spectra of **1–9** show two peaks at about 910 cm^{-1}, reflecting the asymmetric *cis*-dioxo structure [24,25]. In spite of the *trans* structure described in the literature, a *cis* geometry for the dioxomolybdenum core is found for **9** [10]. The other peaks correspond to the vibrational signals of the bound ligands. The Raman spectra exhibit a strong band at ca. 890 cm^{-1} for the symmetric MoO_2-stretching vibration [26].

Crystals of compound **2** suitable for X-ray diffraction were obtained from a saturated chloroform solution. Common to most of the structurally characterized oxomolybdenum compounds of the type MoO_2L_2, the coordination geometry of the molybdenum center in **2** is described best as distorted octahedral (Fig. 2) [15].

Two mutually *trans* oriented alkoxy ligands form the apex, the *cis*-dioxo unit and the nitrogen atoms of the pyridine rings form the equatorial plane of the octahedron. The average bond distance in the *cis*-dioxo group (171.2 pm) is in good agreement with compounds **7** (170.3 pm) and **8** (170.9 pm) [15]. Changes in the substitution pattern of the α-carbon atoms of the alkoxy groups result in different steric demand of the whole pyridyl alcohol ligands and hence in slightly different orientation of these ligands towards each other. In **2**, where the α-carbon atom has two ethyl groups, the N–Mo–N angle amounts to 82.5°, whereas it is 92° in **7** as a result of the increased steric demand of the bulkier phenyl substituents. A survey of important angles and bond lengths is given in Table 4.

The oxo ligands of the complexes **1–9** form a *cis*-dioxo unit, known for all $[MoO_2]^{2+}$ complexes,

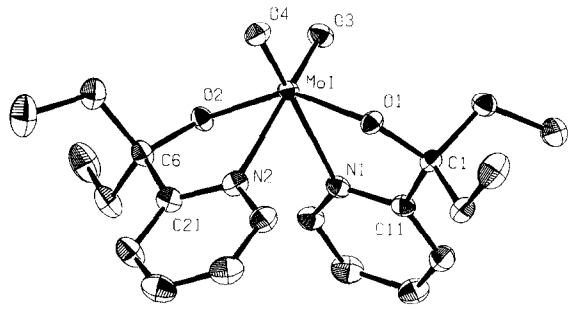

Fig. 2. X-ray structure of **2**.

Table 4
Selected bond lengths and angles

	Distances (pm)		Angles (°)
Mo-O(1)	193.6(1)	O(3)–Mo–O(4)	105.93 (7)
Mo-O(2)	193.0(2)	O(3)–Mo–O(1)	104.54(7)
Mo-O(3)	171.1(2)	O(3)–Mo–O(2)	97.05(7)
Mo-O(4)	171.2(1)	O(3)–Mo–N(2)	165.47(7)
Mo-N(1)	233.9(2)	O(1)–Mo–O(4)	95.89(7)
Mo-N(2)	235.8(2)	O(1)–Mo–N(2)	81.71(6)
C(1)-O(1)	142.7(3)	O(2)–Mo–N(2)	71.86(6)
C(6)-O(2)	142.9(3)	N(1)–Mo–O(4)	164.47(6)
C(11)-N(1)	134.2(3)	N(1)–Mo–O(1)	72.09(6)
C(21)-N(2)	133.6(3)	N(1)–Mo–O(2)	83.19(6)
C(11)-C(1)	152.5(3)	N(1)–Mo–N(2)	82.46(6)
C(21)-C(6)	152.6(3)	Mo–O(1)–C(1)	126.1(1)
		Mo–O(2)–C(6)	126.1(1)
		O(1)–C(1)–C(11)	108.0(2)
		O(2)–C(6)–C(21)	107.9(2)
		C(1)–C(11)–N(1)	114.0(2)
		C(6)–C(21)–N(2)	114.1(2)
		C(11)–N(1)–Mo	114.0(1)
		C(21)–N(2)–Mo	113.6(1)

whereas the nitrogen atoms of the pyridine rings are positioned *trans* to the oxo ligand each. The alkoxy functions of the ligands are placed perpendicular to the plane defined by the dioxomolybdenum core. This could be explained by a *trans* influence of the oxo ligands.

2.3. Catalytic oxidation

At the beginning of our work on molybdenum(VI) complexes our aim was to change the product distribution of the autoxidation reaction of alkenes in favour of the corresponding epoxide. This part of our work based on the fact that high-valent oxides or their acetylacetonato derivatives can improve the product distribution in the autoxidation process of 1-octene [9]. We wanted to make the unselective autoxidation reaction more selective by adding a molybdenum(VI) catalyst. This seems to be very difficult because of the many existing possible reaction pathways. To check our results, we define two parameters, that can be derived from by analytical data: *product selectivity* and *conversion.*

The *product selectivity* of the epoxide is defined as:

$$\text{product selectivity} = \frac{[\text{epoxide}]}{\Sigma[\text{oxo products}]}$$

The advantage of this *new* term is, that we obtain all the required information about the product distribution in one parameter. If the conversion of 1-octene, which is defined below, is 100% the product selectivity becomes the selectivity data that are normally used in literature.

The *conversion* of 1-octene is defined as

$$\text{conversion} = 1 - \frac{[\text{octene}]}{\Sigma[\text{detect. species}]}$$

Table 5
Catalytic autoxidation reaction

Compound used for catalysis	Product selectivity (%)	Reaction time (min)
Autoxidation conditions = no catalyst	24	205
$MoO_2(acac)_2$ (**10**)	6.9	140
MoO_3	38	200
1	48	200
2	58	160
3	49	180
4	48	190
5	46	210
6	47	200
7	49	250
8	41	135
9	45	360

This conversion is determined by measuring the decrease of 1-octene and by adding up the resulting products during the reaction. We are thus able to do a correct mass balance (which is shown for **2** in Table 7). The testing conditions are 100°C and 1 bar of oxygen pressure, because the autoxidation process starts at 90°C. We chose 1-octene as the standard olefin, for its reactivity pattern is very similar to that of the industrial important propylene. 1-Octene has no ring tension that would activate the double bond in oxidation processes, and there is no additional activating influence by electron donating alkyl groups as in 4-octene. Furthermore, 1-octene is a liquid up to 125°C, so it is easier to handle than propylene. It is important to emphasize that we use no additional solvent in order to exclude any solvent effects on the reaction. The atmosphere above the olefin consists of pure oxygen. The reaction is stopped when 10 ml of oxygen have reacted with 2 ml of 1-octene. After the absorption of the oxygen, the mixture is cooled to room temperature thus quenching the reaction immediately. The reaction mixture is analyzed by gas chromatography. The results of these reactions concerning the product selectivity are referenced in Table 5. In the case of the new synthesized complexes **1–6**, the catalyst can be recovered after the reaction. Catalyst decomposition during the reaction has not been observed.

All data have to be referenced to the product selectivity of the autoxidation reaction, (ca. 24%). Corresponding to these data $MoO_2(acac)_2$ decreases the selectivity by a factor of 4. We therefore

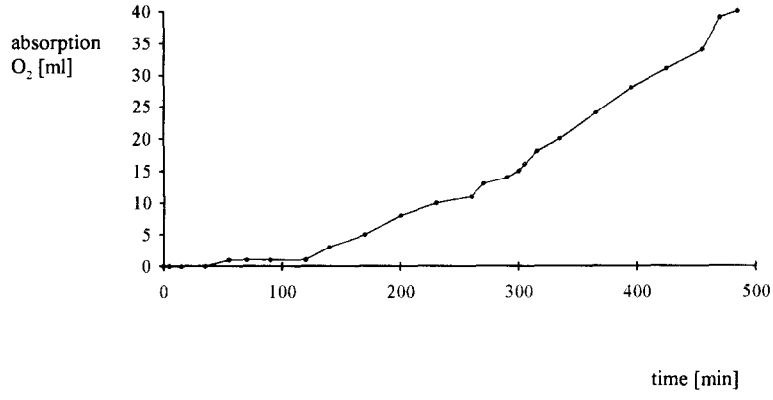

Fig. 3. Oxygen absorption of octene with **2**.

Table 6
Complete product distribution of the catalytic reaction octene, **2**, O_2

Compound	Product selectivity (%)
Cyclooctane	3
Octenol	3
1-Heptanal	4
1-Heptene oxide	4
Octadienol	12
Octenal	14
1-Octene oxide	59
Sum over all products	99

were not able to claim that **10** raises the selectivity [9]. By way of contrast an increase up to 40% with MoO_3 (which is totally insoluble in terminal alkenes) is possible.

Catalytic results of complex **8** are similar to the data of MoO_3. The high selectivity of complex **9** is astonishing since a primary alcohol used as ligand is usually regarded as highly sensitive towards oxidation. Compared to the product selectivity of the rest of the complexes (48%), complex **2** shows the maximum value of 58%.

The catalytic reaction can be carried out with higher turnover numbers with all the complexes **1–9**, if the reaction mixture allowed to convert 40 ml of oxygen instead of 10 ml. The results for the product selectivity are the *same* as in the case of 10 ml oxygen absorbed. The 'best' catalyst **2** shows, i.e., a selectivity of ca. 58%. In all cases the oxygen absorption shows an induction period of about 100 min. After this period slow absorption of oxygen can be observed (Fig. 3).

A product selectivity of about 60% raises the question about the remaining 40% of the oxo products; the complete product distribution for a conversion of 40 ml of oxygen (2 ml 1-octene) with complex **2** is shown in Table 6. The correct mass balance is shown in Table 7.

In Table 7 the sum of all detected species is only 98%, so the missing two percent could be various carboxylic acids, that cannot be detected by means of gas chromatography.

After the presentation of these results two closely related questions should be discussed: (i) why is complex **2** so selective in this reaction, and (ii) is there any link for elucidating the mechanism of this reaction? By adding a radical starter like *tert*-butylhydroperoxide, the reaction is accelerated by a factor of 10 [27]. The product selectivity of the epoxide remains 58% for catalyst **2**. A radical

Table 7
Mass balance of the reaction of **2** with 40 ml O_2

Compound	Mol%
Octene	71
1-Octene oxide	16
Cyclooctane	1
Octenol	1
1-Heptanal	1
1-Heptene oxide	1
Octadienol	3
Octenal	4
Sum over all products	98

inhibitor can be used to stop the reaction immediately. This leads to the conclusion that a radical mechanism should be involved. An additional indication for the radical nature of the reaction is an induction period of about 100 min. Although it is difficult to speculate about the mechanistic details, it is sure that more than one reaction pathway is involved. One is probably a slightly modified radical mechanism according to Schnurpfeil et al. [28,29]:

(a) Attack of the oxygen at the allyl hydrogen atom to form the allyl hydroperoxide; (b) *catalytic* formation of the epoxide and the allylalcohol with the molybdenum(VI) catalyst and the allyl hydroperoxide of (a); (c) oxidative cleavage of the double bond to yield C7 products; (d) oxidation of the allylalcohol.

The product distribution (Table 6) is in good agreement with this mechanism: 3% of the allylalcohol that is formed in step (b), and 4% the cleavage product formed in (c) can be detected. The other products could be described as *oxidative products* of these two by-products.

3. Experimental

All reactions were performed with standard Schlenk techniques in an oxygen-free nitrogen atmosphere. Solvents were dried with standard methods and distilled under N_2. Infrared spectra were recorded on a Perkin-Elmer 1600 series FT-IR spectrometer. The ^{1}H and ^{13}C NMR spectra were recorded at 399.65 and 100.53 MHz on a FT Jeol GX 400 instrument. The ^{17}O and the ^{95}Mo NMR spectra were recorded at 54.22 and 26.06 MHz on a Bruker DPX 400 spectrometer. Elemental analyses were performed in the Microanalytical Laboratory of the Hoechst-Central Research. Molybdenylacetylacetonate MoO_2acac_2 **10**, pyridylmethanol **9a**, butyllithium and 2-bromopyridine were used as received from Aldrich.

3.1. X-ray structure

X-ray structure of compound **2**: colorless crystals of **2** were grown from $CHCl_3$ by slow evaporation. A crystal of the approximate dimensions $0.3 \times 0.2 \times 0.2$ mm was selected in a perfluorinated oil and mounted in a sealed glass capillary on an automated four-cycle X-ray diffractometer (ENRAF-NONIUS CAD4, graphite-monochromatized MoK_α). Crystallographic data are given in Table 8. Final lattice parameters were obtained from 25 machine-centered high angle reflections ($39.9° < 2\Theta < 46.9°$). The range of measurement was $2° < 2\Theta < 50°$ using the ω-scan method, scan width $(0.95 + 0.2 \tan \Theta)°$ ($\pm 25\%$) before and after each reflection to determine the background. Intensity data of 4012 reflections were collected (h, k, $\pm l$), 3352 independent reflections with $I > 0.01 * \sigma(I)$ were used for the refinement. Data were corrected for Lorentz and polarization effects, empirical absorption correction based on Ψ-scan data was applied [30] (transmission coefficients 0.894–0.999), anomalous dispersions was accounted for, the compound showed no significant decomposition during the course of data collection. The structure was solved by direct methods and refined using standard least-squares and subsequent difference Fourier techniques until all atom positions were located. All non-hydrogen atoms were independently refined with anisotropic thermal parameters, all hydrogen atoms were refined isotropically. Refinement of 356 least-squares parameters was continued until the shift/esd ratio was lower than 0.00003 in the last cycle of refinement. All calculations were performed on a DECstation 5000/25 using the programs CRYSTALS [31] and PLATON [32]. Further details of the crystal structure investigation can be obtained from the Fachinformationszentrum Karlsruhe, D-76344 Eggenstein-Leopoldshafen (Germany) on quoting the depository number CSD-405968, the names of the authors, and the journal citation.

Table 8
Crystal structure determination

Formula	$MoO_4N_2C_{20}H_{28}$
Color	colorless
M_r ($g\,mol^{-1}$)	456.4
Crystal system	monoclinic
Space group	$P2_1/c$ (No.14)
Temperature (°C)	−80
a (pm)	1444.5(2)
b (pm)	1052.4(1)
c (pm)	1511.5(2)
β (°)	115.86(1)
V (10^6 pm^3)	2068
D_{calc}($g\,cm^{-3}$)	1.466
Z	4.00
$F(000)$	944.00
μ (cm^{-1})	6.6
λ (pm)	71.073 (MoK_α)
Diffractometer	CAD4 (Enraf Nonius)
2Θ range (°)	$2 < 2\Theta < 50$
Absorption correction	empirical
Data measured	4012
Unique data	3352
Reflections used	3352
$I/\sigma(I)$ limit	0.01
No. of parameters	356
Resid. electron dens.($e\,Å^{-3}$)	+0.27/−0.34
R [a]	0.0284
R_w [b]	0.0215

[a] $R = \Sigma(||F_o| - |F_c||)/\Sigma|F_o|$.
[b] $R_w = [\Sigma w(|F_o| - |F_c|)^2/\Sigma w|F_o|^2]^{1/2}$ with weighting scheme $w = 1/\sigma^2_{(Fo)}$.

3.2. General procedures

3.2.1. Synthesis of the ligands

100 ml diethyl ether are cooled down to −78°C. After addition of 100 mMol of a 1.6 N butyllithium solution in hexane to the cooled ether a clear yellow solution is formed. 95 mMol of 2-bromopyridine in 25 ml diethyl ether are added to the yellow solution over a period of 15 minutes. While adding the 2-bromopyridine the color of the solution changes from yellow to dark red. After stirring at −78°C for 15 minutes the mixture is allowed to warm up to −20°C. Now 105 mMol of the ketone are added. After stirring for 2 hours the solution, that is now slight orange-brown is allowed to warm up to room temperature. After careful hydrolysis, the ether phase is extracted with 5 * 20 ml of 2n hydrochloric acid. After neutralization of the water phase with NaOH, the phase is extracted with diethyl ether. The ether phase is dried with magnesium sulfate and evaporated. A brown oily liquid results, which can be filtered over basic Al_2O_3 to obtain colorless crystals in the case of **1** and **6**, **7**, **8** or a colorless liquid in all other cases.

3.2.2. Synthesis of the molydenum(VI) complexes *1–9*

1.5 g (4.6 mMol) of molybdenylacetylacetonate (**10**) is suspended in 20 ml dried methanol. After addition of 10 mMol of the respective pyridyl alcohol ligand the reaction mixture is stirred for 30 minutes. After 10 minutes the color of the suspension is changing from deep orange to pale orange.

The methanol is evaporated to 10 ml and the remaining methanol is filtered with a zeolithe filter. The pale orange solid is washed two times with cold diethyl ether and dried in vacuo.

3.2.3. Catalytic test

A temperable vessel closed with a reflux condenser is filled with 2 ml 1-octene, 0.2 ml of heptane as internal standard and 1 mol% of the respective catalyst. The atmosphere above the solution is changed from air to pure oxygen. The mixture is heated up to 100°C and the reaction is allowed to go on until 10 or 40 ml of oxygen, respectively, is absorbed. The reaction is quenched by cooling down to room temperature and analysed by GC/FID.

3.3. Analytical data of the molybdenum(VI) complexes

3.3.1. Bis{N,O-[2-(2'-pyridyl)propan-2-olato]}dioxomolybdenum(VI) (1)

Anal. calcd. for $MoO_4N_2C_{16}H_{20}$: C, 48.01; H, 5.04; N, 7.00; O, 15.99; Mo, 23.97; found: C, 47.92; H 5.31; N, 6.99; O, 15.84; Mo, 23.82.

Spectra: IR [KBr, cm^{-1}]: ν(C–H, arom.) = 3100–3020 (w), ν(C–H, aliph.) = 2990 (m), 2925 (w), ν(C–C, arom.) = 1600 (m), 1480 (m), 1440 (m), ν(Mo = O) = 920 (s), 905 (s); ^{1}H NMR [$CDCl_3$, 399.65 MHz, RT, ppm]: δ = 8.68 (1H, d, 6-Py), 7.80 (1H, dd, 4-Py), 7.36 (1H, d, 3-Py), 7.25 (1H, dd, 5-Py), 1.78 (6H, d, CH_3); ^{13}C NMR [$CDCl_3$, 100.53 MHz, RT, ppm]: δ = 168.66 (py-C2), 146.56 (py-C6), 139.20 (py-C4), 122.92 (py-C3), 120.04 (py-C5), 85.30 (C-OH), 30.27 (CH_3), 27.90 (CH_3); ^{17}O NMR [$CDCl_3$, 54.22 MHz, RT, ppm]: δ = 895 (280 Hz, Mo = O); ^{95}Mo NMR [$CDCl_3$, 26.06 MHz, RT, ppm]: δ = 37 (250 Hz); UV/VIS: l = 22,800 nm, 26,100 nm.

3.3.2. Bis{N,O-[3-(2'-pyridyl)-pentan-3-olato]}dioxomolybdenum(VI) (2)

Anal. calcd for $MoO_4N_2C_{20}H_{28}$: C, 52.39; H, 6.16; N, 6.11; O, 13.97; Mo, 21.37; found: C, 52.41; H, 6.52; N, 6.13; O, 14.11; Mo, 21.01.

Spectra: IR [KBr, cm^{-1}]: ν(C–H, arom.) = 3100–3050 (w), ν(C–H, aliph.) = 2990 (s), 2980 (s), 2880 (m), ν(C–C, arom) = 1600 (s), 1520 (m), 1440 (m), ν(Mo = O) = 920 (s), 900 (s), ν(C–H, d-arom) = 780 (m), 720 (m); ^{1}H NMR [$CDCl_3$, 399.65 MHz, RT, ppm]: δ = 8.74 (1H, d, 6-Py), 7.76 (1H, dd, 4-Py), 7.25 (1H, d, 3-Py), 7.24 (1H, dd, 5-Py), 2.02 (4H, m, CH_2), 1.04 (6H, broad d, CH_3); ^{13}C NMR [$CDCl_3$, 100.53 MHz, RT, ppm): δ = 167.44 (py-C2), 147.32 (py-C6), 138.41 (py-C4), 122.69 (py-C3), 120.66 (py-C5), 90.19 (C–OH), 32.13 (CH_2), 30.21 (CH_2), 8.73 (CH_3), 8.43 (CH_3); ^{17}O NMR [$CDCl_3$, 54.22 MHz, RT, ppm]: δ = 899 (270 Hz, Mo = O); ^{95}Mo NMR [$CDCl_3$, 26.06 MHz, RT, ppm]: δ = 48 (250 Hz); UV/VIS: l = 22 600 nm, 26 200 nm.

3.3.3. Bis{N,O-[4-(2'-pyridyl)heptan-4-olato]}dioxomolybdenum(VI) (3)

Anal. calcd for $MoO_4N_2C_{24}H_{36}$: C, 56.01; H, 7.06; N, 5.45; O, 12.44; Mo, 19.04; found: C, 55.99; H, 7.26; N, 5.41; O, 12.51; Mo, 17.92.

Spectra: IR [KBr, cm^{-1}]: ν(C–H, arom.) = 3100–3020 (w), ν(C–H, aliph.) = 2960 (s), 2940 (m), 2870 (m), ν(C–C, arom.) = 1600 (m), 1480 (m), 1440 (m), ν(Mo = O) = 920 (s), 900, (s); ^{1}H NMR [$CDCl_3$, 399.65 MHz, RT, ppm]: δ = 8.69 (1H, d, 6-Py), 7.76 (1H, dd, 4-Py), 7.25 (1H, d, 3-Py), 7.24 (1H, dd, 5-Py), 2.10–1.2 (12H, m, CH_2), 1.04 (6H, broad d, CH_3); ^{13}C NMR [$CDCl_3$, 100.53 MHz, RT, ppm]: δ = 168.02 (py-C2), 147.30 (py-C6), 138.38 (py-C4), 122.51 (py-C2), 120.60 (py-C5), 90.14 (C–OH), 43.16 (CH_2), 41.31 (CH_2), 17.36 (CH'_2), 16.77 (CH'_2), 14.41 (CH_3); UV/VIS: l = 22 800 nm, 26 400 nm.

3.3.4. Bis{N,O-[2,4-dimethyl-3-(2'-pyridyl)pentan-3-olato]}dioxomolybdenum(VI) (4)

Anal. calcd for $MoO_4N_2C_{12}H_{12}$: C, 41.62; H, 3.50; N, 8.09; O, 18.49; Mo, 28.30; found: C, 41.82; H, 3.42; N, 8.29, O, 18.86.

Spectra: IR [KBr, cm^{-1}]: ν(C–H, arom.) = 3100–3050 (w), ν(C–H, aliph.) = 2960 (m), 2920 (m), ν(C–C, arom) = 1600 (m), 1470 (m), 1440 (m), ν(Mo = O) = 920 (s), 910 (s), ^{1}H NMR [$CDCl_3$, 300 MHz, 20°C]: δ = 8.78 (1H, d, 6-Py), 7.90 (1H, dd, 4-Py), 7.43 (1H, dd, 5-Py), 7.37 (1H, d, 3-Py), 2.45 (2H, m, CH), 0.95 (6H, dd, CH_3), ^{13}C NMR [$CDCl_3$, 100.1 MHz, RT, ppm]: δ = 167.42 (py-C2), 146.59 (py-C6), 138.79 (py-C4), 122.32 (py-C2), 120.68 (py-C5), 89.14 (C–OH), 49.16 (CH), 48.12 (CH), 13.36 (CH_3), 12.42 (CH_3).

3.3.5. Bis{N,O-[5-(2'-pyridyl)nonan-5-olato]}dioxomolybdenum(VI) (5)

Anal. calcd for $MoO_4N_2C_{28}H_{44}$; C, 58.92; H, 7.78; N, 4.91; O, 11.22; Mo, 17.17; found: C, 58.82, H, 8.11; N, 4.97; O, 11.15; Mo, 16.23.

Spectra: IR [KBr, cm^{-1}]: ν(C–H, arom.) = 3100–3020 (w), ν(C–H, aliph.) = 2965 (s), 2960 (s), 2880 (m), ν(C–C, arom.) = 1600 (m), 1480 (m), 1440 (m), ν(Mo = O) = 930 (s), 880 (s); ^{1}H-NMR [$CDCl_3$, 300 MHz, 20°C]: δ = 8.72 (1H, d, 6-Py), 7.75 (1H, dd, 4-Py), 7.26 (1H, d, 3-Py), 7.20 (1H, dd, 5-Py), 2.2–1.1 (12H, m, CH_2), 0.87 (6H, d, CH_3); ^{13}C-NMR ($CDCl_3$, 100.1 MHz, 20°): δ = 168.01 (py-C2), 147.30 (py-C6), 138.37 (py-C4), 122.46 (py-C2), 120.60 (py-C5), 89.96 (C–OH), 40.23 (CH'_2), 38.32 (CH'_2), 26.29 (CH''_2), 26.01 (CH''_2), 23.36 (CH'''_2), 23.19 (CH'''_2), 14.04 (CH_3).

3.3.6. Bis{N,O-[1-(2'-pyridyl)cyclohexan-1-olato]}dioxomolybdenum(VI) (6)

Anal. calcd for $MoO_4N_2C_{22}H_{28}$: C, 58.92; H, 7.78; N, 4.91; O, 11.22; Mo, 17.17; found: C, 58.47; H, 7.78; N, 4.98; O, 11.01; Mo 17.32.

Spectra: IR [KBr, cm^{-1}]: ν(C–H, arom.) = 3100–3020 (w), ν(C–H, aliph.) = 2965 (s), 2960 (s), 2880 (m), ν(C–C, arom.) = 1600 (m), 1480 (m), 1440 (m), ν(Mo = O) = 930 (s), 880 (s); ^{1}H NMR [$CDCl_3$, 399.65 MHz, RT, ppm]: δ = 8.64 (1H, d, 6-Py), 7.92 (1H, dd, 4-Py), 7.42 (1H, d, 3-Py), 7.38 (1H, dd, 5-Py), 2.1–1.6 (10H, m, CH_2); ^{13}C NMR [$CDCl_3$, 100.53 MHz, RT, ppm]: δ = 166.43 (py-C2), 143.76 (py-C6), 138.57 (py-C4), 122.33 (py-C2), 121.01 (py-C5), 88.93 (C–OH), 40.21 (CH_2), 38.43 (CH_2), 26.32 (CH'_2), 26.01(CH'_2), 23.42(CH''_2).

3.3.7. Bis{N,O-[(1,1-diphenyl)-(2-pyridyl)methanolato]}dioxomolybdenum(VI) (7)

Spectra: IR [KBr, cm^{-1}]: ν(C–H, arom.) = 3100–3050 (w), ν(C–C, arom.) = 1600 (m), 1500 (m), 1450 (m), ν(Mo = O) = 925,), 900 (s), ν(C–H, d-arom) = 790 (s), 770 (s) ^{1}H NMR [$CDCl_3$, 300.65 MHz, RT, ppm]: δ = 7.68–7.54 (4H, m), 7.42–7.20 (7H, m), 7.12 (2H, d), 6.68 (1H, dd).

3.3.8. Bis{N,O-[1,1-di-(4'',4'''-tert-butyl)phenyl)-1-(2'-pyridyl)methanolato]}dioxomolybdenum(VI) (8)

Spectra: IR [KBr, cm^{-1}]: ν(C–H, arom.) = 3100–3050 (w), ν(C–H, aliph.) = 2980 (s), 2900 (m), 2880 (m), ν(C–C, arom) = 1600 (m), 1520 (m), 1470 (m), ν(Mo = O) = 925 (s), 908 (s); ^{1}H NMR [$CDCl_3$, MHz, RT, ppm]: δ = 7.63–7.50 (3H, m), 7.42–7.20 (4H, m), 7.12 (2H, d), 6.68 (1H, dd); 1.23 (18H, d, CH_3); ^{13}C NMR [$CDCl_3$, 100.53 MHz, RT, ppm]: δ = 165.09, 150.94, 150.11, 148.28, 144.12, 143.72, 137.50, 128.78, 128.07, 128.01, 126.94, 124.93, 124.83, 124.13, 122.10, 122.12, 34.60 (CCH_3), 31.28 (CH_3).

3.3.9. Bis{N,O-[1-(2'-pyridyl)methanolato]}dioxomolybdenum (9)

Anal. calcd for $MoO_4N_2C_{12}H_{12}$, C 41.62, H 3.50, N 8.09, O 18.49, Mo 28.30, found: C, 41.36; H, 3.52; N, 7.88.

Spectra: IR [KBr, cm^{-1}]: ν(C–H, arom.) = 3050–3010 (w), ν(C–H, aliph.) = 2960–2840 (w), ν(C–C, arom.) = 1600 (m), 1458 (m), 1440 (m), ν(Mo = O) = 930 (s), 910 (s), 900 (s); ^{1}H NMR [$CDCl_3$, 399.65 MHz, RT, ppm]: δ = 8.54 (1H, d, 6-Py), 7.76 (1H, dd, 4-Py), 7.31 (1H, d, 3-Py), 7.27 (1H, dd, 5-Py), 5.81 (2H, s, CH_2); ^{13}C NMR [$CDCl_3$, 100.53 MHz, RT, ppm]: δ = 162.08 (py-C2), 146.78 (py-C6), 138.92 (py-C4), 123.28 (py-C3), 119.56 (py-C5), 76.28 (C–OH).

4. Spectroscopic data of the ligands

*4.1. 2-(2'-Pyridyl)propan-2-ol (**1a**)*

^{1}H NMR [$CDCl_3$, 399.65 MHz, RT, ppm]: δ = 8.51 (1H, d, 6-Py), 7.69 (1H, dd, 4-Py), 7.41 (1H, d, 3-Py), 7.17 (1H, dd, 5-Py), 5.20 (1H, broad s, OH), 1.55 (6H, s, CH_3).

*4.2. 3-(2'-Pyridyl)pentan-3-ol (**2a**)*

^{1}H NMR [$CDCl_3$, 399.65 MHz, RT, ppm]: δ = 8.52 (1H, d, 6-Py), 7.70 (1H, dd, 4-Py), 7.28 (1H, d, 3-Py), 7.18 (1H, dd, 5-Py), 5.24 (1H, s, OH), 1.85 (4H, m, CH_2), 0.68 (6H, t, CH_3).

*4.3. 4-(2'-Pyridyl)heptan-4-ol (**3a**)*

^{1}H NMR [$CDCl_3$, 399.65 MHz, RT, ppm]: δ = 8.50 (1H, d, 6-Py), 7.68 (1H, dd, 4-Py), 7.30 (1H, d, 3-Py), 7.16 (1H, dd, 5-Py), 5.30 (1H, s, OH), 1.80 (4H, m, C(3/5)H_2), 1.40 (2H, m, C(2/6)H_2), 0.88 (2H, t, C(2/6)H_2), 0.82 (6H, t, CH_3).

*4.4. 2,4-Dimethyl-3(2'-pyridyl)pentan-3-ol (**4a**)*

^{1}H NMR [$CDCl_3$, 399.65 MHz, RT, ppm]: δ = 8.52 (1H, d, 6-Py), 7.66 (1H, dd, 4-Py), 7.26 (1H, d, 3-Py), 7.19 (1H, dd, 5-Py), 5.60 (1H, s, OH), 2.30 (2H, dt, CH), 0.79 (2H, dd, CH_3).

*4.5. 5-(2'-Pyridyl)nonan-5-ol (**5a**)*

^{1}H NMR [$CDCl_3$, 399.65 MHz, RT, ppm]: δ = 8.50 (1H, d, 6-Py), 7.70 (1H, dd, 4-Py), 7.30 (1H, d, 3-Py), 7.18 (1H, dd, 5-Py), 5.30 (1H, s, OH), 1.80 (4H, m, C(4/6)H_2), 1.35 (2H, m, C(3/7)H_2), 1.20 (4H, m, C(2/8)H_2), 0.80 (2H, m, C(3/6)H_2),0.79 (6H, t, CH_3).

*4.6. 1-(2'-Pyridyl)cylohexan-1-ol (**6a**)*

^{1}H NMR [$CDCl_3$, 399.65 MHz, RT, ppm]: δ = 8.48 (1H, d, 6-Py), 7.66 (1H, dd, 4-Py), 7.44 (1H, d, 3-Py), 7.14 (1H, dd, 5-Py), 5.02 (1H, s, OH), 2.0-1.6 (10H, m, CH).

*4.7. 1,1-Diphenyl-1-(2'-pyridyl)methanol (**7a**)*

Spectra: IR [KBr, cm^{-1}]: ν(C–H, arom.) = 3100–3010 (m), ν(C–C, arom.) = 1600 (m), 1500 (m), 1460 (m), ν(C–H, d-arom.) = 770 (m), 760 (m); ^{1}H NMR [$CDCl_3$, 399.65 MHz, RT, ppm]: δ = 8.57 (1H, d, 6-Py), 7.62 (1H, dd, 4-Py), 7.3-7.18 (11H, d, Phen + 3-Py), 7.12 (1H, dd, 5-Py), 4.5 (1H, broad s, OH).

4.8. 1,1-Di-(4'',4'''-tert-butyl)phenyl)-1-(2'-pyridyl)methanol (8a)

Spectra: IR [KBr, cm^{-1}]: ν(C–H, arom.) = 3100–3010 (m), ν(C–H, arom.) = 2986 (m), ν(C–C, arom.) = 1600 (m), 1500 (m), 1460 (m), ν(C–H, d-arom.) = 770 (m), 760 (m); ^{1}H NMR [$CDCl_3$, 399.65 MHz, RT, ppm]: δ = 8.52 (1H, d, 6-Py), 7.62 (1H, dd, 4-Py), 7.3–7.1 (11H, d, Phen + 3-Py), 7.05 (1H, dd, 5-Py), 4.5 (1H, broad s, OH), 1.22 (18H, s, CH_3).

4.9. Hydroxymethyl-2-pyridine (9a)

^{1}H NMR [$CDCl_3$, 399.65 MHz, RT, ppm]: δ = 8.32 (1H, d, 6-Py), 7.54(1H, dd, 4-Py), 7.28 (1H, d, 3-Py), 7.02 (1H, dd, 5-Py), 5.69 (1H, s, OH), 4.63 (2H, s, CH_2).

5. Conclusion

The new molybdenum(VI) complexes MoO_2L_2 of pyridyl alcohols (L) have led to a better understanding of the oxometal-catalyzed autoxidation of olefins. Contrary to the common opinion, the metal oxidation state of the catalyst is *not* the only factor for the product selectivity in epoxidation [33]. The detailed architecture of the ligand has an important influence on the catalytic performance, too. Selectivity improvements from 38 to 58% have been achieved for the epoxidation of 1-octene with elemental oxygen. Experiments employing radical starters suggest that a radical-type mechanism is operative in this reaction. Further work in this area is under way.

References

[1] R.A. Sheldon, R. Ugo and D. Reidel, Aspects in Homogeneous Catalysis by Metal Complexes (Kluwer, Dordrecht, 1981).
[2] L. Simandi, Catalytic Activation of Dioxygen by Metal Complexes (Kluwer, Dordrecht, 1992).
[3] E.M. Kirschner, Chem. Eng. News (Washington) 73(15) (1995) 16–22.
[4] W.A. Herrmann (Editor), Organic Peroxygen Chemistry, Top. Curr. Chem. 164 (1993).
[5] J.T. Groves and R. Quinn, J. Am. Chem. Soc. 107 (1985) 5790–5792.
[6] R.A. Sheldon, Metalloporphyrins in Catalytic Oxidation Reactions (Marcel Decker, New York, NY, 1994).
[7] B. Scharbert, E. Zeisberger and E. Paulus, J. Organomet. Chem. 493 (1995) 143–147.
[8] W.A. Herrmann, B. Scharbert and G.M. Lobmaier, DEP 4447232.3 (1996).
[9] D. Schnurpfeil, Wiss. Z. TH Leuna Merseburg 27 (1985) 282–294.
[10] R.L. Kelly and Z. Dawoodi, Polyhedron 5 (1986) 271–275.
[11] W. Kaim and B. Schwedrski, Bioinorganic Chemistry: Inorganic Elements in the Chemistry of Life (Wiley, Chichester, 1994).
[12] D. Schnurpfeil and K. Jaky, J. Prakt. Chem. 334 (1992) 165–175.
[13] T.J. Collins, Acc. Chem. Res. 27 (1994) 279–285.
[14] (a) H. Gilman and S.M. Spatz, J. Org. Synth. 74 (1952) 4828. (b) H. Gilman and S.M. Spatz, J. Org. Synth. 74 (1952) 5828. (c) H. Gilman and S.M. Spatz, J. Org. Synth. 74 (1952) 5851.
[15] R.H. Holm, B.E. Schultz, S.F. Geller, M. Muetterties and J.M. Scott, J. Am. Chem. Soc. 115 (1993) 2714–2722.
[16] R.H. Holm, E. Harlan and J. Berg, J. Am. Chem. Soc. 108 (1986) 6992–7000.
[17] R.H. Holm, Chem. Rev. 87 (1987) 1401–1449.
[18] W.A. Herrmann, G. Lobmaier and B. Scharbert, DEP 4447233.1 (1996), Hoechst AG.
[19] J.-P. Kintzinger, Oxygen NMR in NMR, Basic Principles and Progress, Oxygen-17 and Silicon-29 (Springer, Berlin, 1981).
[20] M.A. Freeman, F.A. Schultz and C.N. Railey, Inorg. Chem. 21 (1982) 567–576.
[21] O.V. Klimov, M.A. Fedetov and A.N. Startsev, J. Catal. 139 (1993) 142–152.
[22] M.Minelli, J.E. Enemark, R.T.C. Brownlee, M.J. O'Connor and A.G. Wedd, Coord. Chem. Rev. 68 (1985) 169–278.
[23] K.P. Christensen, P.E. Miller, M. Minelli, T.W. Rockway and J.H. Enemark, Inorg. Chem. Acta 56 (1981) L27.
[24] J.T. Spence, J.H. Enemark, M. Bruck and C. Hinshaw, Inorg. Chem. 28 (1989) 4483–4491.
[25] F.W. Moore and R.E. Rice, Inorg. Chem. 7 (1968) 2510–2514.

[26] J.M. Sobchak, T. Glowiak and J.J. Ziolkowski, Trans. Met. Chem. 15 (1990) 208–211.
[27] H. Mimoun, P. Chaumette and L. Sausine, J. Organomet. Chem. 250 (1983) 291–310.
[28] D. Schnurpfeil and W. Pritzkow, Autoxidation von Kohlenwasserstoffen (VEB Leipzig, 1980).
[29] W. Pritzkow, R. Radeglia and W. Schmitt-Renner, J. Prakt. Chem. 321 (1979) 813–826.
[30] B.A. Frenz, The ENRAF-Nonius CAD4 SDP System (Delft Univ. Press, Delft, 1978).
[31] D.J. Watkin, P.W. Betteridge and J.R. Carruthers, CRYSTALS User Manual (Oxford Univ. Computing Lab., Oxford, 1986).
[32] A.L. Spek, The EUCLID package in Computational Crystallography (Clarendon Press, Oxford, 1982).
[33] E.S. Gould and M. Rado, J. Catal. 12 (1969) 238–244.